JACS
JOURNAL OF THE AMERICAN CHEMICAL SOCIETY
Article
pubs.acs.org/JACS

Synthesis of Isocyanate-Based Brush Block Copolymers and Their Rapid Self-Assembly to Infrared-Reflecting Photonic Crystals

Garret M. Miyake, Raymond A. Weitekamp, Victoria A. Piunova, and Robert H. Grubbs*

Arnold and Mabel Beckman Laboratories for Chemical Synthesis, Division of Chemistry and Chemical Engineering, California Institute of Technology, Pasadena, California 91125, United States

ABSTRACT: The synthesis of rigid-rod, helical isocyanate-based macromonomers was achieved through the polymerization of hexyl isocyanate and 4-phenylbutyl isocyanate, initiated by an *exo*-norbornene functionalized half-titanocene complex. Sequential ruthenium-mediated ring-opening metathesis polymerization of these macromonomers readily afforded well-defined brush block copolymers, with precisely tunable molecular weights ranging from high (1512 kDa) to ultrahigh (7119 kDa), while maintaining narrow molecular weight distributions (PDI = 1.08−1.39). The self-assembly of these brush block copolymers to solid thin-films and their photonic properties were investigated. Due to the rigid architecture of these novel polymeric materials, they rapidly self-assemble through simple controlled evaporation to photonic crystal materials that reflect light from the ultra-violet, through the visible, to the near-infrared. The wavelength of reflectance is linearly related to the brush block copolymer molecular weight, allowing for predictable tuning of the band gap through synthetic control of the polymer molecular weight. A combination of scanning electron microscopy and optical modeling was employed to explain the origin of reflectivity.

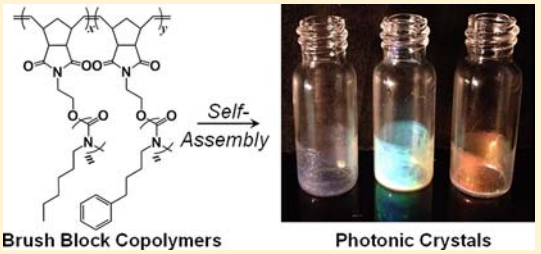

INTRODUCTION

Urbanization is causing a cascade of negative effects on the environment.[1] A readily apparent example on a local scale is the urban heat island (UHI) effect, the phenomenon that urban areas often have higher local temperatures than surrounding areas.[2] A major cause of UHIs is the absorption and thermalization of solar energy by modern building materials. A tremendous amount of money and energy is consumed toward cooling in these areas,[3] resulting in increased pollution[4] and degraded living conditions.[5] To minimize the negative effects of urbanization on the environment, great efforts have been directed toward urban design and the development of new technologies. Because the majority of solar energy is in the form of infrared (IR) radiation, there is strong interest in developing IR-reflecting materials to prevent absorption and thermalization.

Photonic crystals (PCs) are periodic composite materials with frequency-specific reflection, which can be tuned to efficiently reflect IR light.[6] In these materials, the propagation of certain wavelengths of light is forbidden due to photonic band gaps that originate from the periodic modulation of the dielectric function. The wavelength of reflected light is related to the optical path length of the domains, which is determined by the size and refractive index of the components. PCs are most commonly synthesized through layer-by-layer depositions, lithography, or the self-assembly of colloidal crystals.[6] Unfortunately, these routes are expensive or impractical as large area PCs; a more desirable IR-reflective building material would be fabricated inexpensively from a commodity material, such as a polymer. In this context, the self-assembly of block copolymers (BCPs)[7] provides an attractive means to IR-reflecting PCs because of their low cost potential in terms of both raw material and bottom-up fabrication via self-assembly. However, most BCP PCs can only reflect short wavelengths of visible light.[8,9] This is because high molecular weight (MW) polymers, capable of forming large domains, exhibit extreme polymer chain entanglement that is detrimental to self-assembly and inhibits the formation of large, ordered morphologies. To overcome the inability of utilizing high MW BCPs to form polymer PCs that reflect long wavelengths of light, the domain sizes can be enlarged through swelling with additives, namely solvent molecules[10] or homopolymers,[11] although these approaches generally require complicated annealing procedures.

We recently reported that brush BCPs can self-assemble to long-wavelength-reflecting PCs without the need for swelling agents.[12] By exploiting the advantageous characteristics (i.e., livingness, stability, as well as steric and functional group tolerance) of ruthenium (**1**)-mediated ring-opening metathesis polymerization (ROMP)[13] we were able to synthesize well-defined brush BCPs constructed from lactide- and styrene-macromonomers (MMs).[12,14] This "grafting-through" polymerization strategy of MMs affords highly uniform brush BCPs,[15] where the sterically encumbered array of low MW side chains greatly inhibits chain entanglement and forces the unifying main chain to assume a highly elongated conformation.[16] As a result, these brush BCPs rapidly self-assembled to stacked lamellae of alternating layers of lactide and styrene domains, forming one-dimensional (1D) PC architectures. Through controlled evaporation, the films exhibited a maximum peak

Received: July 2, 2012
Published: August 14, 2012

dx.doi.org/10.1021/ja306430k | *J. Am. Chem. Soc.* 2012, 134, 14249−14254

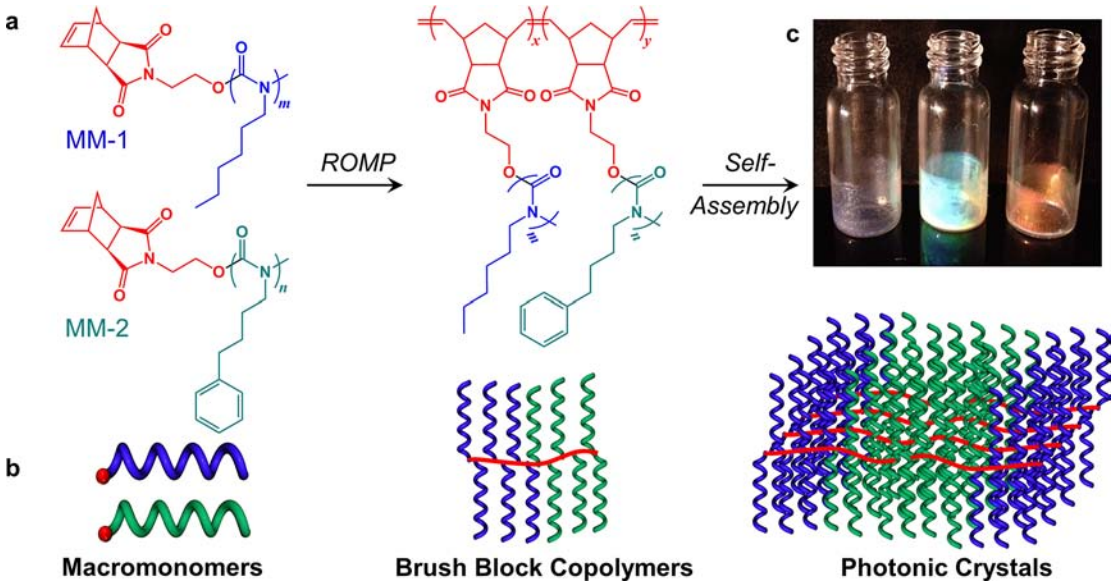

Figure 1. (a) Structures of isocyanate-based macromonomers and their ROMP to brush block copolymers. (b) Schematic representation of the synthesis of brush block copolymers from rigid-rod helical macromonomers and their self-assembly toward 1D photonic crystals. (c) Photograph of photonic crystals reflecting violet, green, and red light.

wavelength (λ_{max}) of reflectance as long as 540 nm, while thermal annealing under compression allowed ultrahigh MW brush BCPs to self-assemble to PCs that reflected light as long as 1311 nm. Although the reported brush BCPs can assemble to IR-reflecting PCs after thermal annealing, we sought to develop a system that could assemble to such domain sizes under ambient conditions to enable widespread applications, including IR-reflecting paints. We envisioned that increasing the rigidity of the grafts would enhance the overall persistence length of the brush BCP, further decreasing chain entanglement and promoting more rapid self-assembly of ultrahigh MW BCPs to even larger domains. Reported herein is the synthesis of brush BCPs constructed from rigid isocyanate-based MMs and their rapid self-assembly through controlled evaporation to PCs that can reflect light from the UV, through the visible, and into the near-IR (Figure 1).

RESULTS AND DISCUSSION

Synthesis of Macromonomers and Brush (Block) Copolymers. Polyisocyanates are a class of polymers that adopt rigid helical secondary structures,[17] and in the case of brush copolymers composed of a polystyrene main chain and polyhexyl isocyanate side chains, it has been shown that the rigid side chains result in main chain elongation, compared to similar graft copolymers with random coil side chains.[18] Thus, we found isocyanate-based MMs to be ideal candidates to investigate if increased side chain rigidity would facilitate self-assembly to large domain sizes and long-wavelength reflecting PCs. Additionally, the controlled polymerization of isocyanates has been well established by Novak and co-workers utilizing half-titanocene (IV) alkoxide initiators, where the alkoxide group is quantitatively incorporated as a chain-end group on the polyisocyanate, providing an efficient means to prepare appropriately functionalized MMs.[19] Embracing Novak's synthetic approach, an *exo*-norbornene half-titanocene derivative (**2**) was conveniently prepared in good yield from the reaction between $CpTiCl_3$ and *N*-(hydroxyethyl)-*cis*-5-norbornene-*exo*-2,3-dicarboximide in the presence of Et_3N. Complex **2** was subsequently employed to produce *exo*-norbornene functionalized MMs from hexyl isocyanate (HICN, MM-1) and 4-phenyl butyl isocyanate (PBICN, MM-2). These MMs exhibited similar MWs (weight average MW (M_w) = 6.77 and 5.99 kDa for MM-1 and MM-2, respectively) and narrow molecular weight distributions (MWDs) (polydispersity index (PDI = M_w/M_n) = 1.05 and 1.07 for MM-1 and MM-2, respectively). The ROMP of MM-1 and MM-2 initiated by **1** was efficient, and could be carried out over a broad range of [MM]:[**1**] ratios, achieving high MM conversion, producing high MW copolymers with narrow MWDs (Table 1). Closer examination of the ROMP of MM-1 shows that it exhibits living characteristics (i.e. linear increase in MW with increasing

Table 1. Results of the ROMP of Macromonomers Mediated by 1.[a]

run no.	MM	[MM]/[1]	time (min)	conv (%)[b]	M_w (kDa)[b]	PDI (M_w/M_n)[b]
1	MM-1	50	50	98.5	364.9	1.03
2	MM-1	100	50	95.8	924.9	1.10
3	MM-1	150	70	95.7	1944	1.11
4	MM-1	200	90	97.0	2123	1.38
5	MM-1	250	150	93.7	3310	1.39
6	MM-2	150	100	90.7	1100	1.07

[a]Polymerizations performed in 3.01 mL of THF at ambient temperature. [MM-1] = [MM-2] = 9.81 mM. [b]Determined by light scattering.

Chart 1. Structures of initiators and monomers utilized in this study

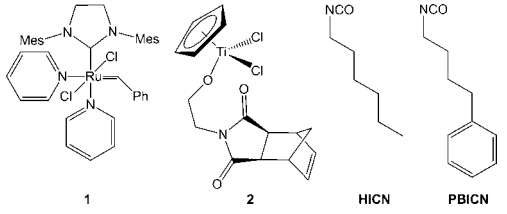

dx.doi.org/10.1021/ja306430k | J. Am. Chem. Soc. 2012, 134, 14249−14254

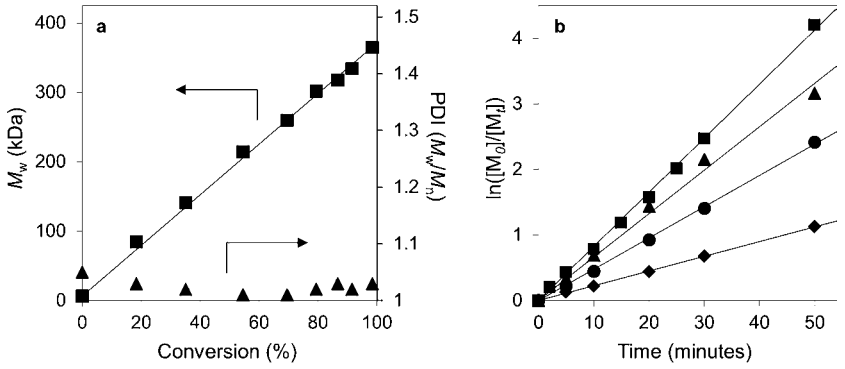

Figure 2. (a) Plot of M_w and PDI as a function of MM-1 conversion ([MM-1]:[**1**] = 50:1). (b) Semilogarithmic plots of ln([MM-1$_0$]/[MM-1$_t$]) as a function of time for the ROMP of MM-1 by **1**. Conditions: [MM-1] = 9.81 mM; [**1**] = 19.7 μM (■), 9.85 μM (▲), 6.57 μM (●), or 3.94 μM (◆). Polymerizations performed in THF at ambient temperature.

MM conversion, and a nearly constant PDI during the course of polymerization) necessary for successful synthesis of well-defined BCPs in a one-pot synthetic procedure (Figure 2a).

A similarly controlled ROMP of MM-2 was observed, although sluggish in comparison to the ROMP of MM-1. Nonetheless, ROMP of MM-2 reached high MM conversion, producing the well-defined brush copolymer (Run, 6, Table 1). To enable the production of well-defined brush BCPs a thorough characterization of the kinetic profile for the ROMP of the MMs is required. The kinetic study of the ROMP of MM-1 reveals a first-order dependence on [MM-1] for all [MM-1]:[**1**] ratios investigated (Figure 2b). Establishing the kinetic profile for the ROMP of MM-1 mediated by **1**, we proceeded to synthesize well-defined BCPs by addition of MM-2 after the ROMP of MM-1. The brush BCPs could be isolated in high yields, with MWs ranging from high (1512 kDa) to ultrahigh (7119 kDa), while maintaining impressively low PDIs (PDI = 1.08−1.39), especially when taking into consideration the magnitudes of the MWs (Table 2). All BCPs had nearly equal molar incorporation of each MM.

Table 2. Results of the Block Copolymerization of Isocyanate Macromonomers Mediated by 1.[a]

run no.	[MM-1]:[MM-2]:[**1**]	time (min)[b]	yield (%)[c]	M_w (kDa)[d]	PDI (M_w/M_n)[d]	MM-1 (mol %)[e]	λ_{max} (nm)[f]
7	100:100:1	48	89.7	1512	1.08	52.4	334
8	150:150:1	64	86.7	2918	1.15	50.8	511
9	200:200:1	85	91.5	4167	1.20	49.9	664
10	215:215:1	94	85.4	5319	1.32	51.3	802
11	250:250:1	144	93.9	7119	1.39	52.3	1120

[a]Polymerizations performed in 3.01 mL of THF at ambient temperature. [MM-1] = [MM-2] = 9.81 mM. [b]Reaction time for polymerization of MM-1. Polymerization was allowed to proceed for 3 (runs 7−9) or 5 (runs 10 and 11) hours after the addition of MM-2. [c]Isolated yield. [d]Determined by light scattering. [e]Determined by ^{1}H NMR. [f]Maximum peak wavelength of reflectance of the primary reflection for films prepared from the controlled evaporation from DCM.

Self-Assembly and PC Properties of Brush BCPs. With a series of well-defined brush BCPs in hand, we began the investigation into the ability of these polymers to rapidly self-assemble to PCs. Thin films of the polymers were prepared through controlled evaporation from DCM, THF, $CHCl_3$, or toluene. In contrast to the previously reported lactide/styrene brush BCPs, no significant solvent effect was observed on self-assembly, as judged by the nearly identical reflectance spectra and λ_{max} of the films. The self-assembly of these brush BCPs to ordered thin-films is dictated through a delicate interplay of factors, including solvent, kinetics, polymer interactions, as well as polymer/substrate interactions.[20] Our preliminary explanation for the negligible solvent effect is that the rigid architecture of the isocyanate brush BCPs promotes a highly elongated main chain, minimizing solvent as well as polymer interactions. This represents a degree of preorganization, which accelerates self-assembly to ordered morphologies. As such, films prepared from the controlled evaporation of DCM solutions were analyzed because it is the most volatile solvent and most strongly highlights the rapid self-assembly of the brush BCPs. The rapid self-assembly of the brush BCPs is qualitatively observed in that the samples with MWs of 1512, 2918, and 4167 kDa produced films that visually appeared violet, green, and red, respectively.

To quantitatively measure the PC properties of these materials, reflectance measurements were acquired as a function of wavelength using a spectrophotometer with an 'integrating sphere' diffuse reflectance accessory (Figure 3a). As expected, the violet, green, and red polymer films showed primary reflectance peaks with λ_{max} = 334, 511, and 664 nm, respectively. It is important to note that the magnitude of reflectance is directly related to the number of layers in the 1D

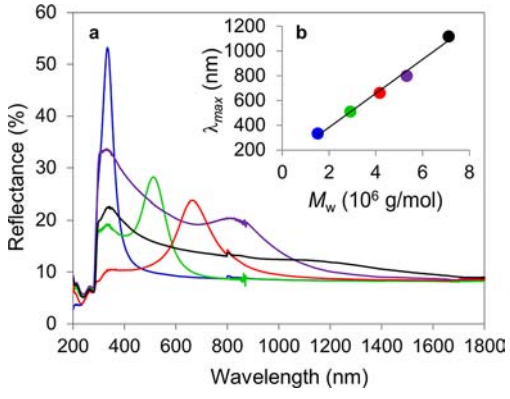

Figure 3. (a) Plot of reflectance as a function of wavelength for isocyanate-based brush BCP thin films with M_w = 1512 (blue), 2918 (green), 4167 (red), 5319 (purple), and 7119 (black) kDa. (b) Plot of λ_{max} as a function of M_w. Color scheme corresponding to M_w is consistent with (a).

dx.doi.org/10.1021/ja306430k | J. Am. Chem. Soc. 2012, 134, 14249−14254

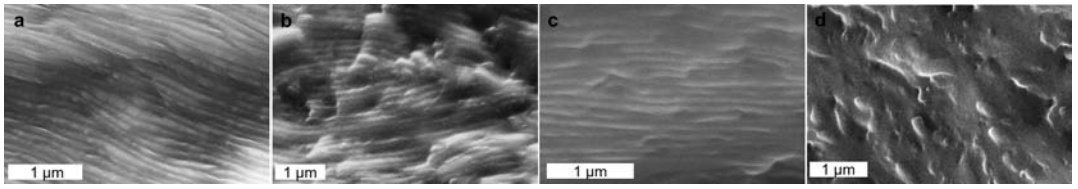

Figure 4. SEM images of cross sections of brush block copolymers with M_w = 1512 (a), 2918 (b), 4167 (c), and 5319 (d) kDA. The perspective places the glass substrate parallel with the text.

PC. Therefore, as the thickness of the film was not strictly controlled, a variation in percent reflectance was observed. In theory, optimization of the layer thickness can lead to 100% reflectance at the appropriate wavelength. The brush BCP with the next highest MW (5319 kDa) in the series exhibited two broad reflectance peaks at 329 and 801 nm. In the case of the ultrahigh MW BCP (M_w = 7119 kDa), extremely broad reflectance was seen extending from 1800 to 300 nm, with a λ_{max} of the primary reflection peak estimated at the plateau with λ_{max} = 1120 nm. Although the broad signals in the reflection spectrum suggest poor self-assembly, the ability to produce broadly reflecting materials could be highly desirable in an IR-reflecting building material. The possibility that the domain sizes of the films could be swollen from residual solvent is eliminated because the film properties are unchanged after being dried under vacuum overnight and are stable over the course of at least months at ambient conditions.

For comparison, with the lactide/styrene brush BCPs, the highest MW polymer that was able to self-assemble through controlled evaporation to a PC structure had a MW of 2940 kDa, with λ_{max} = 540 nm. Thus, the reflectance data clearly shows that the isocyanate-based brush BCPs are superior in regards to facile self-assembly to PCs. Specifically, under less strenuous self-assembly conditions, ultrahigh MW (>7000 kDa) isocyanate-based brush BCPs can reflect light with λ_{max} = 1120 nm, more than 580 nm longer than the lactide/styrene system. Closer inspection of the primary reflection peaks reveals a highly linear correlation between λ_{max} of this peak with increasing MW of the brush BCP (R^2 = 0.990), which is in accord with our earlier reported lactide/styrene brush BCP PCs (Figure 3b). As λ_{max} is directly determined by the domain sizes, this observation shows that, within the window of our investigations, there is a linear increase in domain sizes with increasing BCP MW. In contrast, most linear BCPs exhibit a nonlinear increase in domain size with increasing MW that scales theoretically as $MW^{2/3}$.[21] Thus, the rigid architecture and inhibited chain entanglement of brush BCPs maintains structural integrity as they self-assemble into ordered morphologies, which allows larger domain sizes to be accessed with fewer number of monomer repeat units than their linear counterparts. This predictability in reflectance enables these PCs to be easily incorporated into a variety of specific applications, because the reflectance can be readily tuned through the synthetic manipulation of the polymer MW.

To assign the morphology of the brush BCPs and gain insight into the origin of their PC properties, scanning electron microscopy (SEM) was performed on cross sections of the films to directly image the polymer domains (Figure 4). For the brush BCPs with M_w < 4167 kDa, stacked lamellar morphologies are observed, as expected for BCPs composed of nearly equal ratios of each block (Figure 4a–c). This also explains the origin of the reflective properties of the brush BCPs, as alternating multilayers are the basis for 1D PCs. Most impressively, this order was simply achieved through the rapid self-assembly by controlled evaporation from volatile DCM. Thus, the well-ordered morphologies still accessed by the brush BCPs with MW up to 4167 kDa explain the ability of these polymers to reflect such long wavelengths of light. In contrast, in the lactide/styrene system, thermal annealing was required to self-assemble high MW polymers to equally ordered morphologies. Additionally, with that system, a variation in layer thickness and morphological order was observed as a function of distance from the glass substrate. However, with the current isocyanate-based brush BCPs, the layer thickness and lamellae ordering were uniform throughout the film, regardless of distance from the glass substrate, further demonstrating the drastic beneficial effects that the rigid grafts have on the self-assembly of the brush BCPs to PCs.

When the polymer MW was increased further, unordered morphologies lacking any well-defined domains were observed in the SEM analysis (Figure 4d). This lack of order clearly explains the broad reflectance peaks observed. However, the unordered morphologies revealed by SEM brings forth the question as to how the linear relationship between λ_{max} and BCP MW still holds true with these ultrahigh MW polymers. Investigations toward this answer through vapor and thermal annealing have been unsuccessful at increasing the morphological order, which we currently attribute to the inhibited self-assembly of these ultrahigh MWs.

To further support the proposed origin of reflectivity, the polymer nanostructures were modeled using transfer matrix simulations (Figure 5).[22] An initial guess of the size of each block domain was made using the first order peak of reflection, from the equation $\lambda_{max} = 2(n_1x_1 + n_2x_2)$, using the measured refractive indices of the corresponding brush homopolymers by ellipsometry. A coefficient of variation (CV) for the layer thickness was introduced to account for the increased bandwidth of the reflection peaks due to size dispersity and

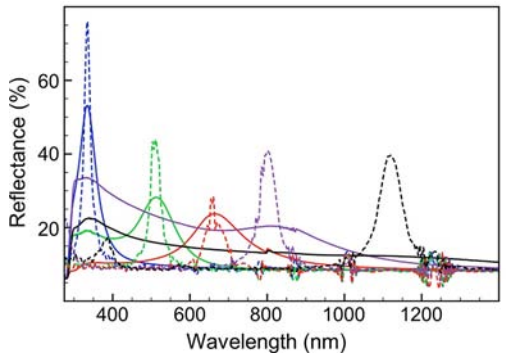

Figure 5. Plot of reflectance as a function of wavelength for isocyanate-based brush BCP thin films with M_w = 1512 (blue), 2918 (green), 4167 (red), 5319 (purple), and 7119 (black) kDa (solid), and the corresponding simulated spectra (dashed).

disorder in the nanostructure (see SI for full modeling details). The CV for the layer thicknesses was set at 10%—this single free parameter provides a method of accounting for the effect of lamellae size distribution on the line widths of the optical spectra. The reflectance spectra of the highest molecular weight samples are broad and no longer resemble the simulated spectra, as expected from the SEM data. Our modeling supports the conclusion that these lamellar nanostructures represent 1D photonic crystals.

CONCLUSION

In conclusion, a series of well-defined (PDI = 1.08−1.39) isocyanate-based brush block copolymers have been synthesized with high (1512 kDa) to ultrahigh (7119 kDa) molecular weights. Due to the rigid-rod secondary structure of the isocyanate grafts, the self-assembly of these block copolymers is enhanced, such that they rapidly form well-ordered morphologies composed of stacked lamellae with large domain sizes. As the domain sizes are directly controlled by the polymer molecular weights, the wavelength of reflectance can be synthetically and predictably tuned from the UV to the near IR by manipulation of the polymer chain length. Visualization of the polymer morphology through SEM and optical modeling confirm that the origin of the reflective properties of these novel polymers is through their assembly into 1D photonic crystal architectures. We believe that because these IR reflecting materials can be fabricated through the evaporation from a volatile solvent under ambient conditions, they show promise as a new technology toward IR-reflective coatings that can be applied as paints.

EXPERIMENTAL SECTION

Materials and Methods. $(H_2IMes)(PPh_3)_2(Cl)_2RuCHPh$ was received as a research gift from Materia Inc. and converted to **1** via literature procedure.[23] All other chemicals were purchased from Sigma Aldrich. Solvents were purified by passage through solvent purification columns and further degassed with argon.[24] Hexyl isocyanate and 4-phenylbutyl isocyanate were dried over CaH_2 overnight and vacuum distilled. *N*-(hydroxyethyl)-*cis*-5-norbornene-*exo*-2,3-dicarboximide was prepared according to literature procedure.[25]

All reactions were carried out in flamed Schlenk-type glassware on a dual-manifold Schlenk line or in a nitrogen-filled glovebox. NMR spectra were recorded on a Varian Inova 300 MHz spectrometer. Chemical shifts were referenced to internal solvent resonances and are reported as parts per million relative to tetramethylsilane. High resolution mass spectra were provided by the California Institute of Technology Mass Spectrometry Facility. Polymer molecular weights were determined utilizing THF as the eluent by multiangle light-scattering (MALS) gel permeation chromatography (GPC) using a miniDAWN TREOS light-scattering detector, a Viscostar viscometer, and an OptilabRex refractive index detector, all from Wyatt Technology. An Agilent 1200 UV−vis detector was also present in the detector stack. Absolute molecular weights were determined using d*n*/d*c* values calculated by assuming 100% mass recovery of the polymer sample injected into the GPC. Polymer thin films were prepared from the controlled evaporation of polymer solutions (∼1.5 g/L) in dichloromethane onto glass slides that had been previously washed with methanol and hexane. After the solvent was allowed to evaporate, the samples were dried under vacuum overnight. SEM images were taken on a ZEISS 1550 VP Field Emission SEM. Reflection measurements were performed on a Cary 5000 UV/vis/NIR spectrophotometer, equipped with an 'integrating sphere' diffuse reflectance accessory (Internal DRA 1800). All measurements were referenced to a LabSphere Spectralon 99% certified reflectance standard. The samples were illuminated through a Spectralon-coated aperture with a diameter of 1 cm, with a beam area of approximately 0.5 cm^2. The samples were scanned at a rate of 600 nm/min, with a 1 nm data interval, from 1800 to 200 nm, with a detector crossover (InGaAs to PMT) at 800 nm.

Synthesis of $CpTiCl_2(C_{11}H_{12}NO_3)$ (2). In a glovebox, a 25-mL flask was charged with 483 mg of $CpTiCl_3$ (2.20 mmol), 10 mL of benzene, and a stir bar. To the rapidly stirred solution was added dropwise a solution of *N*-(hydroxyethyl)-*cis*-5-norbornene-*exo*-2,3-dicarboximide (457 mg, 2.20 mmol) and triethyl amine (223 mg, 2.20 mmol) in 10 mL of benzene. The reaction was allowed to stir for 2 h and was then filtered through a glass frit. The volatiles were removed from the filtrate affording a yellow solid. The solid was recrystallized from a toluene/pentane solvent mixture to afford 350 mg (40.7%) of the pure product.

^{1}H NMR (C_6D_6, 300 MHz, 25 °C): δ 6.16 (s, 5H), 5.70 (t, J = 1.86 Hz, 2H), 4.28 (t, J = 5.58 Hz, 2H), 3.40 (t, J = 14.3 Hz, 2H), 3.05−3.03 (m, 2H), 2.29 (d, J = 1.00 Hz, 2H), 1.29−1.21 (m, 2H). ^{13}C NMR (C_6D_6, 75 MHz, 25 °C): δ 177, 138, 120, 78.9, 48.4, 45.8, 43.6, 40.5. HRMS (FAB^+): Calculated: 390.0149; Found: 390.0143.

Poly(hexyl isocyanate) Macromonomer (MM-1). A 10-mL round-bottom flask was charged with 460 mg of **2** (1.18 mmol), 250 μL of THF, and a stir bar. To the stirred suspension was added 6.87 mL of hexyl isocyanate (47.2 mmol, 40 equiv.). The reaction was allowed to proceed for 21 h before being poured into 50 mL of methanol. The polymer was isolated by filtration, redissolved in methylene chloride, and precipitated again into 50 mL of methanol. MM-1 was isolated by filtration and dried under vacuum at ambient temperature to a constant weight (5.53 g, 92.2%).

^{1}H NMR ($CDCl_3$, 300 MHz, 25 °C): δ 6.30 (bs), 4.28 (bs), 3.68 (bs), 3.08 (bs), 2.71 (bs), 1.62 (bs), 1.28 (bs), 1.12−1.01 (m). M_w =6.77 kDa; PDI = 1.05. dn/dc = 0.0829 mL/g.

Poly(4-phenyl butyl isocyanate) Macromonomer (MM-2). A 10-mL round-bottom flask was charged with 445 mg of **2** (1.14 mmol), 250 μL of THF, and a stir bar. To the stirred suspension was added 1.94 mL of 4-phenyl butyl isocyanate (11.3 mmol, 10 equiv.). The reaction was allowed to proceed for 21 h before being poured into 50 mL of methanol. The polymer was isolated by filtration, redissolved in methylene chloride, and precipitated again into 50 mL of methanol. The polymer was isolated by filtration and dried under vacuum at ambient temperature to a constant weight (1.69 g, 84.4%).

^{1}H NMR ($CDCl_3$, 300 MHz, 25 °C): δ 7.31−7.14 (m), 6.29 (bs), 4.20 (bs), 3.72 (bs), 3.25 (bs), 2.59 (bs), 1.63 (bs), 1.29−1.19 (m). M_w = 5.99 kDa; PDI = 1.07. dn/dc = 0.140 mL/g.

Synthesis of Homo-Brush Polymers. A 20-mL vial was charged with a stir bar, 200 mg of MM-1 (29.5 μmol) or 177 mg MM-2 (29.5 μmol), and 3.0 mL of THF. With rapid stirring 10 μL of an appropriate concentration of **1** in THF was quickly added via syringe. For kinetic analysis a 0.2-mL aliquot of the reaction solution was taken at predetermined time intervals and injected into a 2.0-mL septum sealed vial containing a solution of 25 μL of ethyl vinyl ether in 0.7 mL of THF. The aliquot was analyzed by GPC to determine the percent macromonomer conversion by comparing the peaks corresponding to the brush polymer and the unreacted macromonomer. The polymerization was quenched by the addition of 200 μL of ethyl vinyl ether and addition of 25 mL of methanol. The mixture was allowed to stir for 1 h, and the polymer was isolated by filtration and dried under vacuum at ambient temperature to a constant weight.

Homo-Brush Polymer from MM-1: ^{1}H NMR ($CDCl_3$, 300 MHz, 25 °C): δ 5.78 (bs), 3.94−3.3 (m), 3.68 (bs), 3.22 (bs), 1.85−1.45 (m), 1.28 (bs), 1.11−1.01 (bs), 0.87 (bs). dn/dc = 0.0800 mL/g.

Homo-Brush Polymer from MM-2: ^{1}H NMR ($CDCl_3$, 300 MHz, 25 °C): δ 7.35−6.96 (m), 5.67 (bs), 3.91 (bs), 3.67 (bs), 3.25 (bs), 2.57 (bs), 1.52 (bs), 1.27 (bs). dn/dc = 0.143 mL/g.

Synthesis of Brush Block Copolymers. A 20-mL vial was charged with a stir bar, 200 mg of MM-1 (29.5 μmol), and 3.0 mL of THF. With rapid stirring 10 μL of an appropriate concentration of **1** in THF was quickly added via syringe. At predetermined time intervals 177 mg of MM-2 (29.5 μmol) was added as a solid, and the solution was allowed to react as specified in the polymerization tables. The polymerization was quenched by the addition of 200 μL of ethyl vinyl ether and addition of 25 mL of methanol. The mixture was allowed to

stir for 1 h, and the polymer was isolated by filtration and dried under vacuum at ambient temperature to a constant weight. No unreacted macromonomer was present in the isolated brush block copolymer, as determined by GPC analysis.

^{1}H NMR ($CDCl_3$, 300 MHz, 25 °C): δ 7.35−6.96 (m), 5.67 (bs), 4.18−3.33 (m), 3.23 (bs), 2.54 (bs), 1.94−1.42 (m), 1.28 (bs), 1.13−0.99 (m), 0.87 (bs). d*n*/d*c* values for runs 7−11 in Table 2 = 0.128, 0.108, 0.124, 0.110, and 0.0909 mL/g, respectively.

AUTHOR INFORMATION

Corresponding Author

rhg@caltech.edu

Notes

The authors declare no competing financial interest.

ACKNOWLEDGMENTS

This work was supported by the NSF (CHE-1048404). R.A.W. thanks the Resnick Institute for a graduate fellowship.

REFERENCES

(1) (a) Grimm, N. B.; Faeth, S. H.; Golubiewski, N. E.; Redman, C. L.; Wu, J.; Bai, X.; Briggs, J. M. *Science* **2008**, *319*, 756−760. (b) Karl, T. R.; Trenberth, K. E. *Science* **2003**, *302*, 1719−1723.

(2) (a) Peng, S.; Piao, S.; Ciais, P.; Friedlingstein, P.; Ottle, C.; Bréon, F.; Nan, H.; Zhou, L.; Myneni, R. B. *Environ. Sci. Technol.* **2012**, *46*, 696−703. (b) Kalnay, E.; Cai, M. *Nature* **2003**, *423*, 528−531.

(3) (a) Rizwan, A. M.; Dennis, L. Y. C.; Liu, C. *J. Environ. Sci.* **2008**, *20*, 120−128. (b) Akbari, H.; Pomerantz, M.; Taha, H. *Sol. Energy* **2001**, *70*, 295−310.

(4) (a) Crutzen, P. J. *Atmos. Environ.* **2004**, *38*, 3539−3540. (b) Bennett, M.; Saab, A. E. *Atmos. Environ.* **1982**, *16*, 1797−1822.

(5) Patz, J. A.; Campbell-Lendrum, D.; Holloway, T.; Foley, J. A. *Nature* **2005**, *438*, 310−317.

(6) (a) Ge, J.; Yin, Y. *Angew. Chem., Int. Ed.* **2011**, *50*, 1492−1522. (b) Galisteo-López, J. F.; Ibisate, M.; Sapienza, R.; Froufe-Pérez, L. S.; Blanco, Á.; López, C. *Adv. Mater.* **2011**, *23*, 30−69. (c) Wang, J.; Zhang, Y.; Wang, S.; Song, Y.; Jiang, L. *Acc. Chem. Res.* **2011**, *44*, 405−415. (d) Aguirre, C. I.; Reguera, E.; Stein, A. *Adv. Funct. Mater.* **2010**, *20*, 2565−2578. (d) Moon, J. H.; Yang, S. *Chem. Rev.* **2010**, *110*, 547−574.

(7) (a) Bates, F. S.; Hillmyer, M. A.; Lodge, T. P.; Bates, C. M.; Delaney, K. T.; Fredrickson, G. H. *Science* **2012**, *336*, 434−440. (b) Park, C.; Yoon, J.; Thomas, E. L. *Polymer* **2003**, *44*, 6725−6760.

(8) For selected reviews see: (a) Paquet, C.; Kumacheva, E. *Mater. Today* **2008**, *11*, 48−56. (b) Yoon, J.; Lee, W.; Thomas, E. L. *MRS Bull.* **2005**, *30*, 721−726. (c) Edrington, A. C.; Urbas, A. M.; DeRege, P.; Chen, C. X.; Swager, T. M.; Hadjichristidis, N.; Xenidou, M.; Fetters, L. J.; Joannopoulos, J. D.; Fink, Y.; Thomas, E. L. *Adv. Mater.* **2001**, *13*, 421−425. (d) Fink, Y.; Urbas, A. M.; Bawendi, M. G.; Joannopoulos, J. D.; Thomas, E. L. *J. Lightwave Technol.* **1999**, *17*, 1963−1969.

(9) For selected examples see: (a) Hustad, P. D.; Marchand, G. R.; Garcia-Meitin, E. I.; Roberts, P. L.; Weinhold, J. D. *Macromolecules* **2009**, *42*, 3788−3794. (b) Rzayev, J. *Macromolecules* **2009**, *42*, 2135−2141. (c) Runge, M. B.; Bowden, N. B. *J. Am. Chem. Soc.* **2007**, *129*, 10551−10560. (d) Yoon, J.; Mathers, R. T.; Coates, G. W.; Thomas, E. L. *Macromolecules* **2006**, *39*, 1913−1919.

(10) (a) Parnell, A. J.; Pryke, A.; Mykhaylyk, O. O.; Howse, J. R.; Adawi, A. M.; Terrill, N. J.; Fairclough, J. P. A. *Soft Mater* **2011**, *7*, 3721−3725. (b) Kang, C.; Kim, E.; Baek, H.; Hwang, K.; Kwak, D.; Kang, Y.; Thomas, E. L. *J. Am. Chem. Soc.* **2009**, *131*, 7538−7539. (c) Yoon, J.; Lee, W.; Thomas, E. L. *Macromolecules* **2008**, *41*, 4582−4584. (d) Kang, Y.; Walish, J. J.; Gorishnyy, T.; Thomas, E. L. *Nat. Mater.* **2007**, *6*, 957−960.

(11) (a) Urbas, A.; Sharp, R.; Fink, Y.; Thomas, E. L.; Xenidou, M.; Fetters, L. J. *Adv. Mater.* **2000**, *12*, 812−814. (b) Urbas, A.; Fink, Y.; Thomas, E. L. *Macromolecules* **1999**, *32*, 4748−4750.

(12) Sveinbjörnsson, B. R.; Weitekamp, R. A.; Miyake, G. M.; Xia, Y.; Atwater, H. A.; Grubbs, R. H. *P. Nat. Acad. Sci. USA* **2012**, DOI: 10.1073/pnas.1213055109.

(13) (a) Vougioukalakis, G. C.; Grubbs, R. H. *Chem. Rev.* **2010**, *110*, 1746−1787. (b) Leitgeb, A.; Wappel, J.; Slugovc, C. *Polymer* **2010**, *51*, 2927−2946. (c) Bielawski, C. W.; Grubbs, R. H. In *Controlled and Living Polymerizations*. Müller, A. H. E., Matyjaszewski, K., Eds.; Wiley-VCH: Weinheim, Germany. 2009; pp 297−342. (d) Bielawski, C. W.; Grubbs, R. H. *Prog. Polym. Sci.* **2007**, *32*, 1−29. (e) Slugovc, C. *Macromol. Rapid Commun.* **2004**, *25*, 1283−1297.

(14) (a) Xia, Y.; Olsen, B. D.; Kornfield, J. A.; Grubbs, R. H. *J. Am. Chem. Soc.* **2009**, *131*, 18525−18532. (b) Xia, Y.; Kornfield, J. A.; Grubbs, R. H. *Macromolecules* **2009**, *42*, 3761−3766.

(15) Sumerlin, B. S.; Matyjaszewski, K. In *Macromolecular Engineering: Precise Synthesis, Materials Properties, Applications*; Matyjaszewski, K., Gnanou, Y., Leibler, L., Eds.; Wiley-VCH: Weinheim, Germany, 2007.

(16) Hu, M.; Xia, Y.; McKenna, G. B.; Kornfield, J. A.; Grubbs, R. H. *Macromolecules* **2011**, *44*, 6935−6934.

(17) (a) Yashima, E.; Maeda, K.; Iida, H.; Furusho, Y.; Nagai, K. *Chem. Rev.* **2009**, *109*, 6102−6211. (b) Green, M. M.; Park., J.; Sato, T.; Teramoto, A.; Lifson, S.; Selinger, R. L. B.; Selinger, J. V. *Angew. Chem., Int. Ed.* **1999**, *38*, 3138−3154. (c) Mayer, S.; Zentel, R. *Prog. Polym. Sci.* **2001**, *26*, 1973−2013.

(18) Kikuchi, M.; Lien, L. T. N.; Narumi, A.; Jinbo, Y.; Izumi, Y.; Nagai, K.; Kawaguchi, S. *Macromolecules* **2008**, *41*, 6564−6572.

(19) (a) Patten, T.; Novak, B. M. *J. Am. Chem. Soc.* **1996**, *118*, 1906−1916. (b) Patten, T. E.; Novak, B. M. *J. Am. Chem. Soc.* **1991**, *113*, 5065−5066.

(20) Albert, J. N. L.; Epps, T. H. *Mater. Today* **2010**, *13*, 24−33.

(21) Matsen, M. W.; Bates, F. S. *J. Polym. Sci., Part B: Polym. Phys.* **1997**, *35*, 945−952.

(22) Orfanidis, S. J. *Electromagnetic Waves and Antennas*. Online book, retrieved May 2012. http://www.ece.rutgers.edu/~orfanidi/ewa/.

(23) Love, J. A.; Morgan, J. P.; Trnka, T. M.; Grubbs, R. H. *Angew. Chem., Int. Ed.* **2002**, *41*, 4035−4037.

(24) Pangborn, A. B.; Giardello, M. A.; Grubbs, R. H.; Rosen, R. K.; Timmer, F. J. *Organometallics* **1996**, *15*, 1518−1520.

(25) Matson, J. B.; Grubbs, R. H. *J. Am. Chem. Soc.* **2008**, *130*, 6731−6733.